



Modeling, processing, and characterization of exfoliated graphite nanoplatelet-nylon 6 composite fibers



Myungsoo Kim^a, Sang-Ha Hwang^a, Byeong-Joo Kim^a, Jong-Beom Baek^{b,d}, Hyeon Suk Shin^{c,d}, Hyung Wook Park^{a,d,*}, Young-Bin Park^{a,d,*}, Il-Joon Bae^e, Seong-Young Lee^e

^aSchool of Mechanical and Nuclear Engineering, Ulsan National Institute of Science and Technology, UNIST-gil 50, Ulsju-gun, Ulsan 689-798, Republic of Korea

^bSchool of Energy and Chemical Engineering, Ulsan National Institute of Science and Technology, UNIST-gil 50, Ulsju-gun, Ulsan 689-798, Republic of Korea

^cSchool of Natural Science, Ulsan National Institute of Science and Technology, UNIST-gil 50, Ulsju-gun, Ulsan 689-798, Republic of Korea

^dLow-Dimensional Carbon Materials Center, Ulsan National Institute of Science and Technology, UNIST-gil 50, Ulsju-gun, Ulsan 689-798, Republic of Korea

^eCarbon Materials Research Group, Research Institute of Industrial Science and Technology, San 32, Hyoja-dong, Nam-gu, Pohang 790-330, Republic of Korea

ARTICLE INFO

Article history:

Received 27 October 2013

Received in revised form 7 June 2014

Accepted 17 June 2014

Available online 24 June 2014

Keywords:

A. Fibers

A. Nano structures

C. Analytical modeling

E. Melt-spinning

ABSTRACT

We present theoretical and experimental studies on the effects of platelet-like filler orientation on the mechanical properties of melt-spun exfoliated graphite nanoplatelet(xGnP)-nylon 6(PA6) composite fibers. In numerical studies, the Mori–Tanaka micromechanics model was employed to formulate analytical models to predict the mechanical properties of xGnP-PA6 composite fibers with varying xGnP orientations in a three-dimensional spatial domain. Simulation results showed that the predicted properties of xGnP-PA6 composite fibers were highly affected by xGnP orientation and were correlated with the measured properties of composite fibers treated with varying draw ratios. The tensile moduli of composite fibers at varying xGnP contents showed significant improvements, which is attributed to the drawing-induced alignment of PA6 molecular chains as well as the alignment of xGNPs. Both as-received and acid-treated xGNPs were incorporated in PA6, and mechanical test results suggested that acid-treated xGNPs provide stronger interfacial bonding with PA6.

© 2014 Elsevier Ltd. All rights reserved.

1. Introduction

Over the years, functional fibers have received much attention in various applications, including electroactive polymer actuators [1], flame retardant and thermally stable materials [2], bio-scaffolds [3], and energy and storage textiles [4]. In particular, novel functionality or multifunctionality has been integrated into nanocomposite fibers by incorporating the unique material properties of nanoscale fillers, such as carbon nanotubes (CNTs), two-dimensional carbon materials, and montmorillonite [2,5–7].

Modeling polymer composite fibers filled with nanoscale materials to predict their mechanical properties has been a topic of great interest in the composite community [8]. Most existing models employ such micromechanics-based models as Mori–Tanaka and Halpin–Tsai models. In an attempt to predict the stiffness of aligned short-fiber composites, Tucker and Liang [9] evaluated sev-

eral micromechanics models, including Eshelby's equivalent inclusion, self-consistent model for finite-length fibers, Mori–Tanaka model, bounding models, Halpin–Tsai model and its extensions, and shear lag models. They recommended the Mori–Tanaka model as the most accurate predictive model for estimating the stiffness of aligned fiber composites. Their work marked the starting point for several research efforts to follow, which applied the Mori–Tanaka model to predict the mechanical properties of nanocomposites [10–14]. Odegard et al. [10] linked atomistic simulations of CNTs to continuum models of the corresponding composites. They obtained the properties of single-walled carbon nanotube (SWCNT) polymer composites using the Mori–Tanaka model in the combination with SWCNT properties derived from molecular dynamics. Ashrafi et al. [11,12] studied high-speed multifunctional micro-actuators composed of CNT-reinforced composites using the Eshelby–Mori–Tanaka model. They reported that CNT reinforcement enhanced the axial tensile modulus and longitudinal wave velocity of nanocomposite beams.

In addition to nanocomposite fiber modeling, there have been several research efforts devoted to manufacturing composite fibers for characterization, including electrospinning [7,15], melt spinning [2,5], and wet spinning [6]. Mazinani et al. [15] reported that

* Corresponding authors at: School of Mechanical and Nuclear Engineering, Ulsan National Institute of Science and Technology, UNIST-gil 50, Ulsju-gun, Ulsan 689-798, Republic of Korea. Tel.: +82 52 217 2314; fax: +82 52 217 2309.

E-mail addresses: hwpark@unist.ac.kr (H.W. Park), ypark@unist.ac.kr (Y.-B. Park).

the CNTs show a higher degree of alignment in electrospun conductive polyethylene terephthalate/CNT nanocomposite fibers when the nanotube concentration is below the electrical percolation threshold. Hamza et al. [16–18] observed the relationship between the effect of draw ratio and microstructural changes in synthetic fibers by stretching fibers at room temperature and observing changes in the optical properties using an interferometric method. They reported that stretching polypropylene or nylon 6 fibers reduced the size of cross sectional area of the fibers and aligned molecule chains in the stretching direction (parallel to the fiber axis) which increased strength of the fibers. Several researchers investigated stretching effect by increasing draw ratio during manufacturing of polymer nanocomposite fibers [19,20] or films [21] including nano-size fillers, such as MWNTs [19], carbon fibers [20] or graphene oxides [21]. Their experimental data revealed that increasing the draw ratio aligned the molecule chains of polymer and nanofillers along the drawn direction, which led to improvement in tensile modulus and strength parallel to the drawn direction.

Despite numerous studies on modeling of bulk nanocomposites and nanocomposite fibers, there have been limited research efforts devoted to modeling and simulation for prediction of mechanical properties of polymer composite fibers containing two-dimensional carbon nanomaterials, such as graphene or exfoliate graphite nanoplatelets (xGnPs). In addition, most of the work to date manufacturing and characterizing nanocomposite fibers has focused on nanocomposite fibers containing one-dimensional CNTs, whose drawing-induced alignment behavior would be inherently different from two-dimensional fillers.

We present a study on modeling, processing, and characterization of nanocomposite fibers consisting of xGnPs and nylon 6 (or polyamide (PA) 6). Using the Mori–Tanaka model and orientation tensors, the mechanical properties of nanocomposite fibers were predicted at varying filler concentrations and degrees of filler orientation. For experimental verification, as-received and acid-treated xGnPs were incorporated in the polymer to produce melt-spun nanocomposite fibers at varying xGnP concentrations and draw ratios, and their respective tensile properties were compared to investigate the effects of interfacial bonding between xGnPs and PA6, as well as the effects of xGnP loading and orientation.

2. Theoretical

2.1. Orientation of two-dimensional nanomaterials in polymer composites

The orientation of xGnP can be expressed using a unit vector \mathbf{p} in the thickness direction [22–24] as shown in Eq. (1) and Fig. 1.

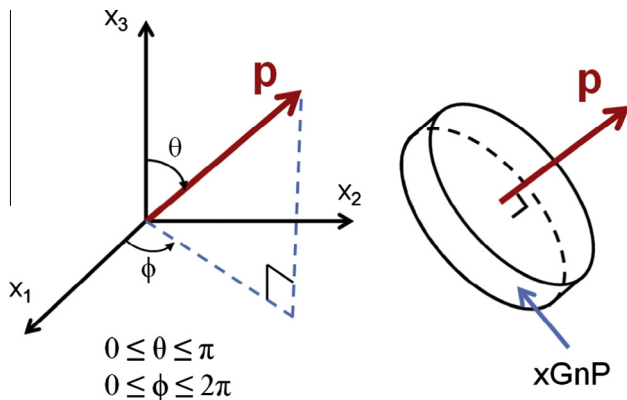


Fig. 1. Coordinate system and definitions of θ , ϕ , and \mathbf{p} .

$$\mathbf{p} = \begin{Bmatrix} \cos \phi \sin \theta \\ \sin \phi \sin \theta \\ \cos \theta \end{Bmatrix} \quad (1)$$

The components of vector \mathbf{p} in Eq. (1) were used to obtain the second- and fourth-rank xGnP orientation tensors (a_{ij} and a_{ijkl}), which were required to obtain the stiffness tensor of a composite. The two orientation tensors are integrations over all possible orientations of the dyadic products of the vector \mathbf{p} components with the distribution function $\psi(\mathbf{p})$. (See Advani and Tucker [22] for details.)

$$\begin{aligned} a_{ij} &= \int_{\mathcal{S}^2} p_i p_j \psi(\mathbf{p}) d\mathbf{p} \\ a_{ijkl} &= \int_{\mathcal{S}^2} p_i p_j p_k p_l \psi(\mathbf{p}) d\mathbf{p} \\ i, j, k, l &\in \{1, 2, 3\} \end{aligned} \quad (2)$$

2.2. Mori–Tanaka model

A stiffness tensor bridges stresses and strains in a constitutive equation, which can be expressed as $\sigma_{ij} = \bar{\mathbf{C}}_{ijkl} \varepsilon_{kl}$, where $i, j, k, l \in \{1, 2, 3\}$, or $\sigma_i = \bar{\mathbf{C}}_{ij} \varepsilon_j$, where $i, j \in \{1, 2, \dots, 6\}$, in a contracted form. The elastic properties of composites, such as tensile modulus, Poisson's ratio, and shear modulus, are obtained from the stiffness tensor [25]. Here, the Mori–Tanaka model was employed to obtain the stiffness tensor of unidirectional (aligned) composites, which is one of the most accurate models for prediction of the mechanical properties of composites [9]. The Mori–Tanaka model can be expressed as Eq. (3) [10–14,26]

$$\bar{\mathbf{C}}_{ijkl} = \mathbf{C}^m + \mathbf{V}_f \langle (\mathbf{C}^f - \mathbf{C}^m) \mathbf{A}^f \rangle (\mathbf{V}_m \mathbf{I} + \mathbf{V}_f \langle \mathbf{A}^f \rangle)^{-1} \quad (3)$$

where $\bar{\mathbf{C}}_{ijkl}$ is stiffness tensor of composite; \mathbf{C}^m and \mathbf{C}^f are stiffness tensors of matrix and filler, respectively, V_m and V_f are volume fractions of matrix and filler, respectively, and \mathbf{I} is identity tensor. The terms enclosed in the angular brackets represent the average over all orientation. The dilute mechanical strain concentration tensor, \mathbf{A}^f , is given by

$$\mathbf{A}^f = [\mathbf{I} + \mathbf{S}(\mathbf{C}^m)^{-1}(\mathbf{C}^f - \mathbf{C}^m)]^{-1} \quad (4)$$

where \mathbf{S} is Eshelby tensor [27,28].

2.3. Stiffness tensor of composites

After obtaining the stiffness tensor of unidirectional composites, the average of the elastic constants of stiffness tensor for partially or randomly aligned composites can be obtained using Eq. (5) [22,24]

$$\begin{aligned} \mathbf{C}_{ijkl} &= B_1(a_{ijkl}) + B_2(a_{ij}\delta_{kl} + a_{kl}\delta_{ij}) + B_3(a_{ik}\delta_{jl} + a_{il}\delta_{jk} + a_{ji}\delta_{ik} + a_{jk}\delta_{il}) \\ &\quad + B_4(\delta_{ij}\delta_{kl}) + B_5(\delta_{ik}\delta_{jl} + \delta_{il}\delta_{jk}) \end{aligned} \quad (5)$$

where δ_{mn} is Kronecker delta (1 if $m = n$, 0 if $m \neq n$), and a_{ij} and a_{ijkl} are the moments of distribution as shown in Eq. (2). B_i 's are five scalar constants obtained from the unidirectional and transversely isotropic stiffness tensor $\bar{\mathbf{C}}_{ijkl}$ in Eq. (3) and can be expressed as Eq. (6) [22]. (See [29] for conversion of the fourth-order tensor to the second-order matrix form.)

$$\begin{aligned} B_1 &= \bar{\mathbf{C}}_{11} + \bar{\mathbf{C}}_{22} - 2\bar{\mathbf{C}}_{12} - 4\bar{\mathbf{C}}_{66} \\ B_2 &= \bar{\mathbf{C}}_{12} - \bar{\mathbf{C}}_{23} \\ B_3 &= \bar{\mathbf{C}}_{66} + \frac{1}{2}(\bar{\mathbf{C}}_{23} - \bar{\mathbf{C}}_{22}) \\ B_4 &= \bar{\mathbf{C}}_{23} \\ B_5 &= \frac{1}{2}(\bar{\mathbf{C}}_{22} - \bar{\mathbf{C}}_{23}) \end{aligned} \quad (6)$$

Download English Version:

<https://daneshyari.com/en/article/7213600>

Download Persian Version:

<https://daneshyari.com/article/7213600>

[Daneshyari.com](https://daneshyari.com)